Mechanics Informed Approach to Online Prognosis of Composite Airframe Element

Stiffness Monitoring with SHM Data and Data-Driven RUL Prediction

Yue, Nan; Galanopoulos, Georgios; Loutas, Theodoros; Zarouchas, Dimitrios

Important note
To cite this publication, please use the final published version (if applicable).
Please check the document version above.

Mechanics Informed Approach to Online Prognosis of Composite Airframe Element: Stiffness Monitoring with SHM Data and Data-Driven RUL Prediction

Nan Yue[1,2](✉) ⓘ, Georgios Galanopoulos[3], Theodoros Loutas[3], and Dimitrios Zarouchas[1,2]

[1] Structural Integrity and Composites Group, Faculty of Aerospace Engineering, Delft University of Technology, Delft, The Netherlands
N.Yue@tudelft.nl

[2] Center of Excellence in Artificial Intelligence for Structures, Prognostics and Health Management, Aerospace Engineering Faculty, Delft University of Technology, Delft, The Netherlands

[3] Applied Mechanics Laboratory, Department of Mechanical Engineering and Aeronautics, University of Patras, 26504 Rio, Greece

Abstract. During the service of composite airframes, damage initiates and accumulates due to the manufacturing imperfections, impact damage and cyclic loadings, leading to the degradation in its load-bearing capacity. The nature of the degradation process is complicated due to the multi-mode damage propagation and complexity in the structural details of airframes. In the condition-based health management of airframe structures, the degradation is expressed in the concept of remaining useful life (RUL). Online prognostic health management is an emerging field dedicated to the timely prediction of RUL using onboard sensors. This work presents a mechanics-informed approach to the prognosis of a typical airframe element, stiffened CFRP composite panel, under compression-compression fatigue. The fatigue degradation of axial stiffness is monitored by Lamb wave velocity and utilised for online RUL prediction via particle filter.

Keywords: Composite · Airframe · Stiffness degradation · Lamb wave · Particle filter · SHM · PHM · RUL

1 Introduction

Stiffened panels are widely used in airframe structures due to their high strength-to-weight ratio [1]. The growing use of high-performance composite materials has further motivated the design of composite stiffened panels [2]. However, composite structures are vulnerable to impact. Impact damage can significantly compromise the strength and fatigue life of stiffened panels, particularly when the impact result in the disbonding of stiffener [3–5]. This susceptibility of composite airframe structures to damage has led to cautious design and maintenance approaches, resulting in overdesigned composite

components that are either prematurely removed from service or repaired more often than necessary. To optimise life management for more a sustainable aviation, prognostic health management has attracted interest from both industry and academia. Online prognostic health management is an emerging field dedicated to the timely prediction of RUL using on-board sensors.

Fatigue degradation of composite materials is a complex multi-scale damage accumulation process. Fatigue of simple composite laminates cause multiple types of micro level damage accumulation such as matrix cracking, fibre-matrix interface disbonding, fibre failure, causing macro scale degradation such as strength and stiffness reduction [6, 7]. In addition to the micro and macro level degradation seen in simple composite coupons, the fatigue of complex composite structures is inevitably complicated by the geometries and complex structural behaviour [8–10].

Online prognosis of complex structures faces many challenges. First of all, an accurate degradation model of a complex structure is often not available. Damage progression models suitable for simple geometries may not be appropriate to complex structures. Even if such model is available, the in-situ measurement of the model input (such as micro-level damage parametres such as matrix crack density) is very challenging. In this case there is a tendency of favouring data-driven methods that do not require a degradation model. However, due to the high cost of testing, produce enough data for training such data-driven method can be time consuming and expensive, therefore is not always an option. Even if a data set is available, data-driven (ML) methods tend to be effective only for the same conditions of training data.

This paper proposes a mechanics informed approach to prognosis of complex airframe structures. This approach leverage the degradation in mechanical behaviour of a complex structure in RUL prediction via interpreting the physical meaning of sensor data for prognostic health indicator. The mechanical properties are assessed periodically using a distributed sensor network permanently installed on the structure. The estimated degradation in mechanical properties then used for RUL prediction via particle filter. The proposed method is demonstrate on composite stiffened panels under compression-compression fatigue until failure.

This paper is organised as follows. Section 2 presents the methodology of Lamb wave based stiffness estimation. Section 3 presents the methodology of RUL prediction using particle filter. Section 4 presents the experimental details. Section 5 presents the result. The paper is concluded in Sect. 6.

2 Lamb Wave Based Stiffness Estimation as Health Indicator

The methodology of Lamb wave based health indicator has been presented in detail in a previous work [11]. For the reader's convenience and the completeness of this paper, the key methodology is presented in this section.

For typical aeronautical grade CFRP composite laminates, the dispersion curve of S0 mode is nearly flat in the low frequency thickness product region, indicating that the phase velocity is almost insensitive to the thickness or frequency, and thus depicts a quasi-nondispersive behavior which is beneficial for material characterization purposes. The use of the S0 mode allows flexibility in the excitation frequency and it is also the

fastest mode which is convenient in practice. Another benefit of using the S0 mode is that the relation of phase velocity and axial young's modulus can be derived at 0 frequency thickness product.

The Young's modulus E can then be estimated using a low frequency S0 mode phase velocity as [12]

$$E = \rho\left(1 - v^2\right)C_p^2 \tag{1}$$

where E, ρ and v are Young's modulus, density and Poisson's ratio of the medium, respectively. Assuming the change in density and Poisson's ratio is negligible, the degradation of the axial modulus can be described by

$$D = \frac{E}{E_0} = \left(\frac{C_p}{C_{p0}}\right)^2 \tag{2}$$

where C_{p0} denote the S0 mode phase velocity at pristine condition.

In the case of mode conversion, S0 mode converts to A0 mode, and the phase velocity of the first arriving wave changes significantly but this change cannot represent the change in modulus. Assuming that the converted A0 mode corresponds to flexural waves in the low frequency domain, according to Kirchhoff theory [13], the modulus E can be estimated as

$$E = \frac{c_g^2}{4k^2\alpha} = \frac{c_p^2}{k^2\alpha} \tag{3}$$

At a given frequency (and thus a given wavenumber k) and under the assumption that α is constant, the stiffness degradation can still be calculated by Eq. 2.

To obtain the correct reference phase velocity value after mode conversion, the reference phase velocity is changed to the first available phase velocity after mode conversion. Referring to Eq. 2, the stiffness degradation can be written as

$$D = \frac{E}{E_0} = \frac{E_1}{E_0} \cdot \frac{E}{E_1} = \left(\frac{C_{pk}}{C_{p0}}\right)^2 \cdot \left(\frac{C_{p1}}{C_{pk+1}}\right)^2 \tag{4}$$

where the subscript 0 denotes the initial wave mode, subscript k denotes the last recording of the initial wave mode, subscript k + 1 denotes the first recording of the converted wave mode, and C_{p1} denotes the phase velocity of the current wave mode. Therefore, the phase velocity ratio after mode conversion can be calculated as $\frac{C_{pk}}{C_{po}} \cdot \frac{C_{p1}}{C_{pk+1}}$.

The axial stiffness of the structure at frequency f is estimated by the mean value of the selected paths:

$$D^f = \overline{D_p^f} \tag{5}$$

where D_p^f denotes the estimated axial stiffness degradation in path p at frequency f.

If multiple Lamb wave frequencies are assessed, he overall stiffness estimation is the average of the stiffness estimation at each frequency weighted by the number of valid signal paths w_f at corresponding frequencies:

$$D = \frac{\sum_f w_f \cdot D_f}{\sum_f w_f} \tag{6}$$

A signal path is considered invalid when its signal-to-noise ratio falls below a certain threshold.

3   Prognosis Using Particle Filter

Particle filtering (PF) is a recursive Bayesian state estimation method that uses a set of discrete weighted samples (particles) to approximate the state distribution of a stochastic process given noisy and/or partial observations [14]. PF is particularly effective in estimating states of nonlinear and/or non-Gaussian systems, and it has been widely used in model-based RUL prognosis [15, 16].

The general state-space model of a system takes the form:

$$x_k = f(x_{k-1}, \theta_{k-1}) + u_k \tag{7}$$

$$y_k = h(x_k) + \upsilon_k \tag{8}$$

where x_k denotes system state, θ_k denotes model parametres, u_k denotes process noise, y_k denotes measurement, υ_k denotes measurement noise, $f(\cdot)$ and $h(\cdot)$ denote the state transfer function and observation function, respectively.

The particle approximation to the state distribution at time k is

$$\boldsymbol{z_k} = \left\{ \left(x_k^i, \theta_k^i \right), \omega_k^i \right\}_{i=1}^{N} \tag{9}$$

where N denotes the number of particles, and for particle i, x_k^i denotes the state estimates, θ_k^i denotes the parametre estimates, and ω_k^i denotes the weight.

The N particles are generated from prior probability density functions, and are assigned equal weights of $\omega_0^i = 1/N$. When a measurement y_k is available at time k, the likelihood of each particle is calculated as

$$p(z_k|y_k) = \frac{1}{\sigma_v\sqrt{2\pi}} \exp\left[-\frac{(y_k - h(x_k))^2}{2\sigma_v^2} \right] \tag{10}$$

where σ_v is measurement uncertainty. The weight of the particle i is updated as

$$\omega_k^i = \omega_{k-1}^i \cdot p\left(z_k^i|y_k \right) \tag{11}$$

Subsequently, the weights are normalized so that the sum of all weights equals 1:

$$\omega_k^i = \frac{\omega_k^i}{\sum_{i=i}^{N} \omega_k^i} \tag{12}$$

To avoid particle degeneracy after updating, the number of effective particles is estimated by

$$N_{eff} = \frac{1}{\sum_{i=i}^{N} (\omega_k^i)^2} \tag{13}$$

Systematic resampling is performed if the number N_{eff} is below a threshold N_T. The weights of the resampled particles are all re-assigned equally.

To allow adaptability of model parameters, a random walk step of model parameters is performed following the updating step:

$$\theta_k = \theta_k + \epsilon, \epsilon \sim N(0, \sigma_\epsilon) \tag{14}$$

After updating, each particle is propagated using Eq. 7 until time $k + l$ when end of life (EOL) criteria is reached:

$$x_{k+l}^i = f(x_k^i, \theta_k^i, e_k^i), i = 1, \ldots, N \tag{15}$$

The remaining useful life estimation of particle i at time k is calculated as

$$RUL_k^i = t_{k+l}^i - t_k^i \tag{16}$$

The distribution of RUL estimation can be skewed so the percentiles are used for prediction interval for robustness to skewness and extreme values. RUL prediction is the weight median/50th percentile of RUL distribution. The uncertainty of the RUL estimation are assessed by 50% interval (25th to 75th weighted percentile) and 90% interval (5th to 95th weighted percentile).

4   Experimental Setup

The dataset used in this work was produced at Delft University of Technology and is available at [17]. Four nominally identical composite stiffened panels are considered. Each specimen consists of a skin panel (300 mm × 165 mm × 1.83 mm) and a co-cured T-stiffener (bonded foot width of 65.5 mm and web width of 46.5 mm), as shown in Fig. 1(a). The skin and stiffener are both made from IM7/8552 unidirectional prepreg in layup sequence of [45/-45/0/45/90/-45/0]s and [45/-45/0/45/-45]s, respectively. Two epoxy resin tabs were moulded around the ends of the panel to distribute compressive load. The dimension of the panel excluding the tab is shown in Fig. 1(b).

The specimens are sensorised with piezoelectric sensors (PZT patches, 20 mm in diameter and 0.5 mm in thickness) on the stiffener side for guided wave acquisition. Eight sensors are surface mounted on each specimen using an appropriate adhesive. Piezo sensors, their gluing process and their electronic conditioning (LWDS) are deliverables from CEDRAT TECHNOLOGIES.

To simulate an impact event in aircraft service conditions, a drop weight impact is performed on the skin side of the panels prior to the fatigue test, resulting in barely visible impact damage (BVID). The damage locations are shown in Fig. 1.
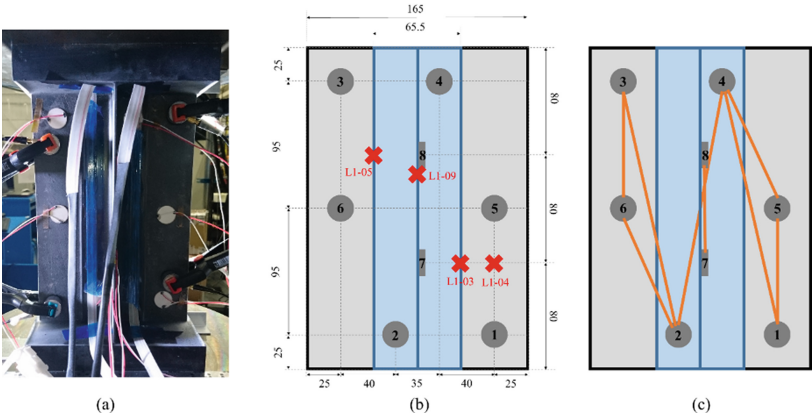
Fig. 1. (a) Stiffened panel; (b) Dimensions (in mm) excluding tab seen from stiffener side. The piezoelectric sensors are marked by grey circles (1 to 8). The impact location on each panel is marked by red crosses. (c) Selected lamb waves paths, marked in orange lines.

Prior to fatigue, the buckling load and ultimate compressive load are assessed with a quasi-static compression test of a pristine panel, which was estimated at 12.8 kN and 104 kN, respectively. The stiffened panels are tested under compression-compression fatigue until failure with maximum load around 65% of the ultimate load with a load ratio of 0.1. The damage locations, compressive load and the number of cycles to failure of four stiffened panels are summarised in Table 1.

Table 1. Summary of test details

Specimen	Damage type	Damage location	Minimum compressive load (kN)	Maximum compressive load (kN)	Cycles to failure
L1-03	10 J impact	Stiffener foot edge	6.5	65	152,458
L1-04		Skin			280,098
L1-05		Stiffener foot edge			144,969
L1-09		Stiffener foot center			133,281

The fatigue load cycle is interrupted every 5000 cycles, and the applied load is reduced to 0.2 kN for Lamb wave measurements. Lamb waves are excited at frequencies of 50, 100, 125, 150, 200, 250 kHz by applying a 5-cycles tone burst signal on one PZT sensor and are acquired using the other PZT sensors. The guided waves signals are recorded in a round robin way, where each PZT acts sequentially as transmitter and receiver. Each signal is recorded 10 times and averaged for noise reduction.

5   Results

This section present the results of Lamb wave based stiffness estimation and RUL prediction.

In the post-buckling compression-compression fatigue, the deflection due to buckling is likely to introduce matrix cracking perpendicular to the loading (axial) direction. Therefore, the signal paths predominantly along the loading axis are selected to assess the axial phase velocity, as shown in Fig. 1(c). Figure 2 shows the pre-processed signals recorded after impact at 0, 5000, 10000 and 15000 C-C fatigue cycles. Two fundamental wave modes can be observed at the first arrival of the signals over the acquired frequency range. The fundamental asymmetric (A0) mode is mainly seen at 50 kHz and the fundamental symmetric (S0) mode exists at higher frequencies. The change in amplitude and phase of the guided wave signals can be observed at all acquired frequencies, while more changes are seen at 50 kHz to 150 kHz compared to 200 kHz and 250 kHz. Considering the stronger response, flexibility in frequency selection, and convenience in material characterization of S0 mode, S0 mode dominant guided waves response at 100 kHz, 125 kHz and 150 kHz are considered in this work, as marked in Fig. 2.
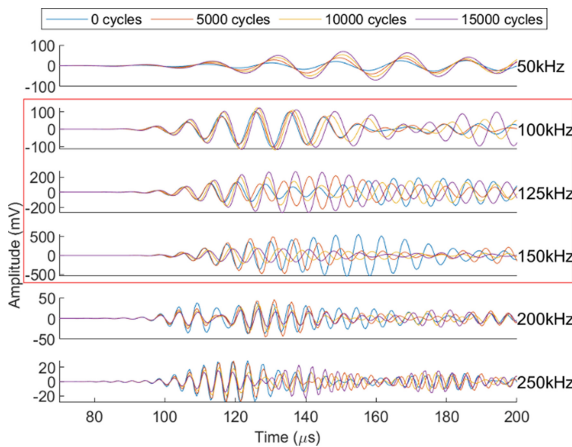

Fig. 2. Lamb wave signals at 0, 5000, 10000, 15000 C-C fatigue cycles recorded by path 1–5 of specimen L1-03. Signals at 100 kHz, 125 kHz and 150 kHz are used in this work (marked with red rectangles).

The stiffness degradation estimation of the four specimens using Lamb waves is shown in Fig. 3. The EOL criteria is set to be the highest failure stiffness, which is 0.945.

A stiffness degradation model is required for RUL prediction. The degradation model should capture the degradation trend while remain a simple form for general applications. In this work, a strictly decreasing linear degradation model is considered:
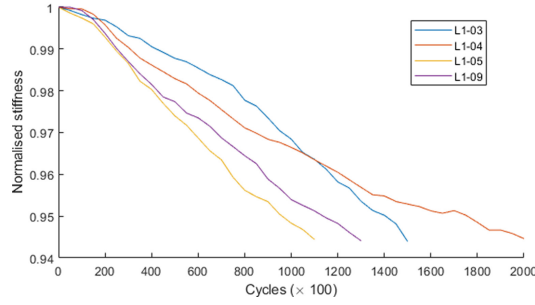
$$x(k) = 1 - a \cdot k, a > 0 \tag{17}$$

Fig. 3. Normalised stiffness degradation estimated using Lamb waves

where a is model parameter. The state transition function is

$$\Delta x(k) = -a + u$$
$$x(k) = x(k-1) + \Delta x(k)$$

$$(18)$$

The prior distribution of model prametre a is determined using Eq. 15 on data presented in Fig. 3, which is $N(0.3752, 0.1028)$. 600 particles are sampled from the prior distrbution. The process noise and measurement noise are sampled from $u \sim N(0, 0.001)$ and $v \sim N(0, 0.001)$, respectively.

Particle filtering is performed at every 100 cycles, and the particle weights are updated every 5000 cycles when Lamb wave measurement is acquired, and a random walk of the model parametre a with 10% of its prior standard deviation is performed after each update. Systematic resampling is performed when the precentage of effective particle number falls below 75%. The history of filtered observation and the parametre evolution of specimen L1-03 is show as an example in Fig. 4.
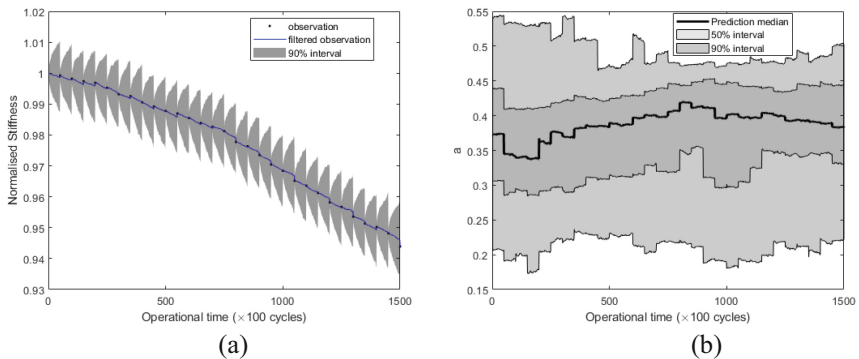

Fig. 4. (a) History of filtered observation. (b) Evolution of model parametre

The RUL is predicted after each update. Figure 5 shows the RUL prediction of the four specimens as function of operational time (the number of fatigue cycles). The prediction median converges to the true RUL and the prediction intervals shrink as operational times increases.
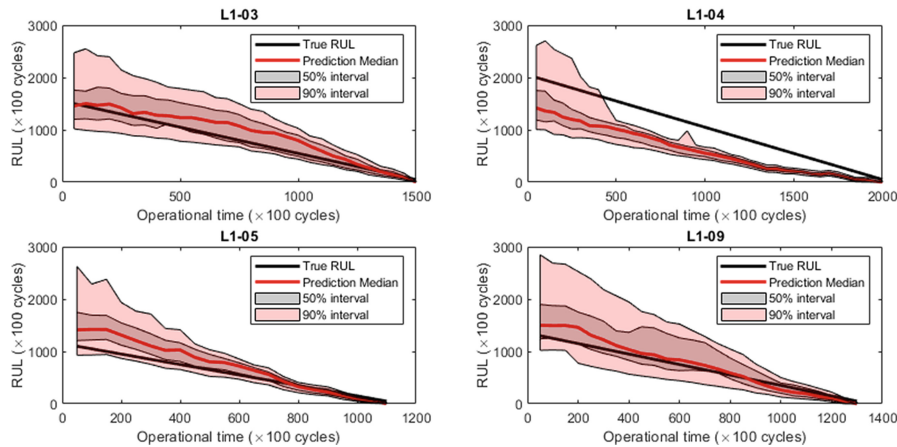

Fig. 5. RUL prediction

The RUL performance is evaluated using performance indices listed in Table 2.

Table 2. RUL performance indices

Error	$e_k = RUL_k^{True} - RUL_k$
Accuracy	$\overline{e_k} = \frac{1}{K}\sum_{k=1}^{K} e_k$
Precision	$\sqrt{\frac{\sum_{k=1}^{K}(e_k - \overline{e_k})^2}{K-1}}$
Mean absolute percentage error (MAPE)	$\frac{1}{K}\sum_{k=1}^{K}\left|\frac{100 \bullet e_k}{RUL_k^{True}}\right|$

The performance indices are summarised in Table 3. The RUL prediction has the best performance in specimen L1-09. The average accuracy and precision are 21800 cycles and 12700 cycles, respectively. The average MAPE is 30.3%.

Table 3. Performance of RUL prediction

	L1-03	L1-04	L1-05	L1-09	Average
Accuracy ($\times$100 cycles)	186	-374	196	114	218
Precision ($\times$100 cycles)	106	164	158	118	137
MAPE (%)	32.8	43.2	29.1	15.9	30.3

6 Conclusion

A mechanics informed approach to online prognosis of complex airframe structures is proposed in this paper. This approach utilises the global fatigue degradation phenomenon of a complex structure for prognosis. The degradation in stiffness is assessed periodically by a distributed piezoelectric sensor network permanently installed on the structure. Particle filter is then used to predict RUL using estimated stiffness. The propose approach achieved good result in a typical composite airframe element, composite panels with T stiffeners, under compression-compression fatigue subjected to impact at various locations.

References

1. Chu, S., Featherston, C., Kim, H.A.: Design of stiffened panels for stress and buckling via topology optimization. Struct. Multidiscip. Optim. **64**(5), 3123–3146 (2021). https://doi.org/10.1007/s00158-021-03062-3
2. Nagendra, S., Jestin, D., Gürdal, Z., Haftka, R.T., Watson, L.T.: Improved genetic algorithm for the design of stiffened composite panels. Comput. Struct. **58**, 543–555 (1996)
3. Greenhalgh, E., Meeks, C., Clarke, A., Thatcher, J.: The effect of defects on the performance of post-buckled CFRP stringer-stiffened panels. Compos. Part A Appl. Sci. Manuf. **34**, 623–633 (2003)
4. Meeks, C., Greenhalgh, E., Falzon, B.G.: Stiffener debonding mechanisms in post-buckled CFRP aerospace panels. Compos. Part A Appl. Sci. Manuf. **36**, 934–946 (2005)
5. Raimondo, A., Riccio, A.: Inter-laminar and intra-laminar damage evolution in composite panels with skin-stringer debonding under compression. Compos. B Eng. **94**, 139–151 (2016)
6. Ansari, M.T.A., Singh, K.K., Azam, M.S.: Fatigue damage analysis of fiber-reinforced polymer composites—a review. J. Reinf. Plast. Compos. **37**, 636–654 (2018)
7. Li, X., Kupski, J., De Freitas, S.T., Benedictus, R., Zarouchas, D.: Unfolding the early fatigue damage process for CFRP cross-ply laminates. Int. J. Fatigue **140**, 105820 (2020)
8. Alderliesten, R.C.: Critical review on the assessment of fatigue and fracture in composite materials and structures. Eng. Fail. Anal. **35**, 370–379 (2013)
9. Abramovich, H., Weller, T., Bisagni, C.: Buckling behavior of composite laminated stiffened panels under combined shear-axial compression. J. Aircr. **45**, 402–413 (2008)
10. Broer, A., Galanopoulos, G., Benedictus, R., Loutas, T., Zarouchas, D.: Fusion-based damage diagnostics for stiffened composite panels. Struct. Health Monit. (2021)

11. Yue, N., Broer, A., Briand, W., Rébillat, M., Loutas, T., Zarouchas, D.: Assessing stiffness degradation of stiffened composite panels in post-buckling compression-compression fatigue using guided waves. Submitted for publication
12. Tao, C., Ji, H., Qiu, J., Zhang, C., Wang, Z., Yao, W.: Characterization of fatigue damages in composite laminates using Lamb wave velocity and prediction of residual life. Compos. Struct. **166**, 219–228 (2017)
13. Grahn, T.: Lamb wave scattering from a circular partly through-thickness hole in a plate. Wave Motion **37**, 63–80 (2003)
14. Goebel, K., Daigle, M.J., Saxena, A., Roychoudhury, I., Sankararaman, S., Celaya, J. R.: Prognostics: the science of making predictions (2017)
15. Cadini, F., Sbarufatti, C., Corbetta, M., Giglio, M.: A particle filter-based model selection algorithm for fatigue damage identification on aeronautical structures. Struct. Control Health Monit. **24**(11), e2002 (2017)
16. Zhang, L., Mu, Z., Sun, C.: Remaining useful life prediction for lithium-ion batteries based on exponential model and particle filter. IEEE Access **6**, 17729–17740 (2018)
17. Zarouchas, D., Broer, A., Galanopoulos, G., Briand, W., Benedictus, R., Loutas, T.: Compression compression fatigue tests on single stiffener aerospace structures. DataverseNL (2021)